

Supporting Information

Fluorescent and energy transfer properties of heterometallic lanthanide-titanium oxo clusters coordinated with anthracenecarboxylate ligand

Sheng Wang, Hu-Chao Su, Lan Yu, Xiao-Wei Zhao, Li-Wen Qian, Qin-Yu Zhu* and Jie Dai*

Table S1. Crystal Data and Structural Refinement Parameters for **1–3**.

Figure S1. FTIR spectra of **1–4**

Figure S2. XRD patterns of the bulk microcrystal samples of **1–4** along with those simulated from the data of single-crystal analysis.

Figure S3. Thermogravimetric analysis of **1–4**.

Figure S4. Molecular structures of **1** (a) and **2** (b) with the ellipsoid presentation.

Figure S5. Ball-stick structures of **3** (a) and **4** (b).

Figure S6. Solid state fluorescence spectra of **2** and **4**, also illustrating the result of energy transfer within the cluster.

Figure S7. Solid state fluorescence spectra of **1** and **2**.

Table S1. Crystal Data and Structural Refinement Parameters for **1–3**.

	1	2	3
formula	C ₇₆ H ₁₂₆ Cl ₂ Nd ₂ N ₂ O ₄₂ Ti ₁₀	C ₇₆ H ₁₂₆ Cl ₂ Eu ₂ N ₂ O ₄₂ Ti ₁₀	C ₆₂ H ₁₂₄ Cl ₂ Nd ₂ O ₄₂ Ti ₁₀
fw	2578.17	2593.61	2379.83
cryst size (mm ³)	0.20 × 0.30 × 0.50	0.20 × 0.30 × 0.50	0.25 × 0.25 × 1.00
cryst syst	triclinic	triclinic	monoclinic
space group	<i>P</i> $\bar{1}$	<i>P</i> $\bar{1}$	<i>P</i> 2 ₁ / <i>n</i>
<i>a</i> (Å)	14.890(3)	14.6136(8)	15.092(3)
<i>b</i> (Å)	14.976(3)	14.7178(8)	17.568(4)
<i>c</i> (Å)	15.484(3)	15.0540(8)	18.631(4)
α (deg)	64.46(3)	64.8600(15)	90.00
β (deg)	77.29(3)	78.1730(15)	91.72(3)
γ (deg)	63.90(3)	64.3150(14)	90.00
<i>V</i> (Å ³)	2795.8(10)	2640.6(2)	4937.5(17)
<i>Z</i>	1	1	2
ρ_{calcd} (g cm ⁻³)	1.531	1.646	1.599
<i>F</i> (000)	1306	1324	2408
μ (mm ⁻¹)	1.707	2.012	1.924
<i>T</i> (K)	293(2)	296(2)	293(2)
reflns collected	25538	57727	26691
unique reflns	12333	12176	11132
observed reflns	6538	9583	8909
GOF on <i>F</i> ²	1.055	1.023	1.198
<i>R</i> ₁ [<i>I</i> >2σ(<i>I</i>)]	0.0786	0.0401	0.0759
<i>wR</i> ₂	0.1466	0.1045	0.1381

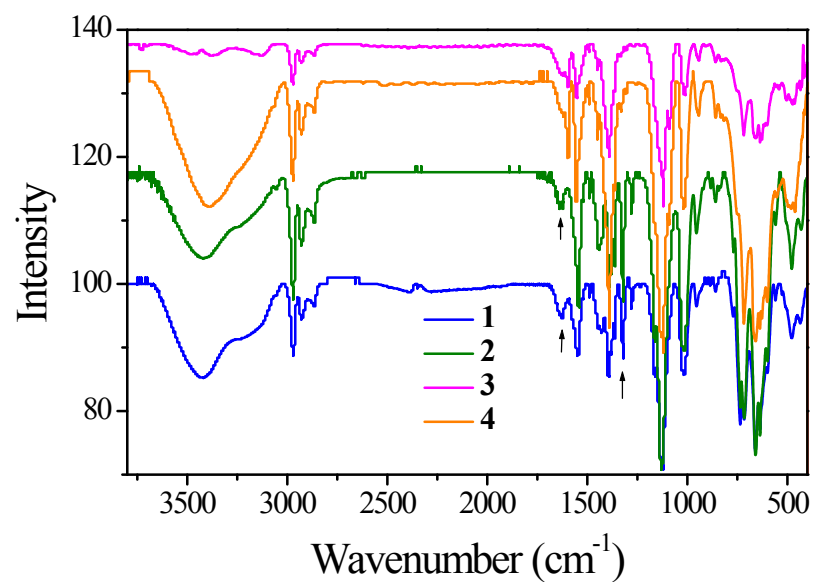
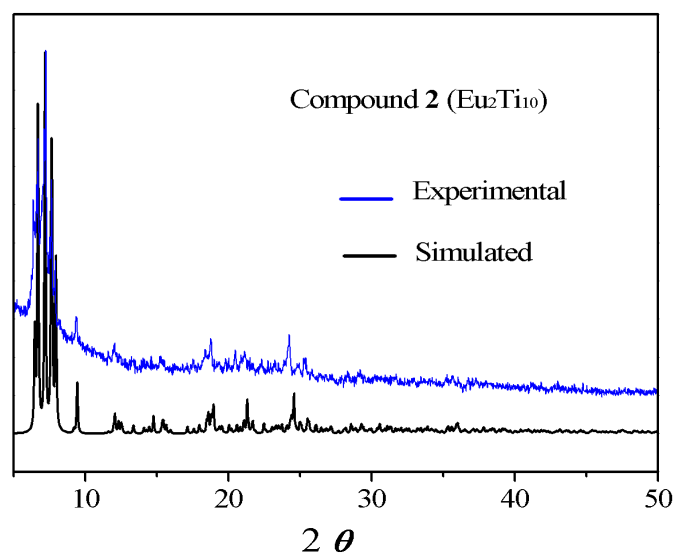
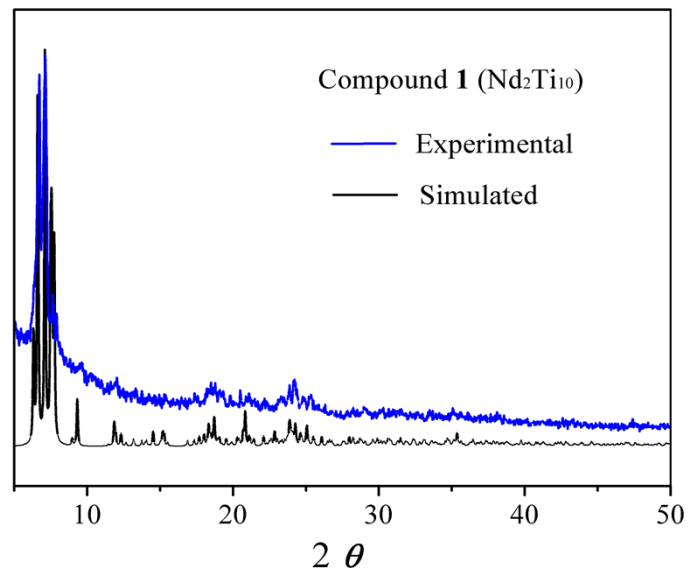


Figure S1. FTIR spectra of **1–4**.



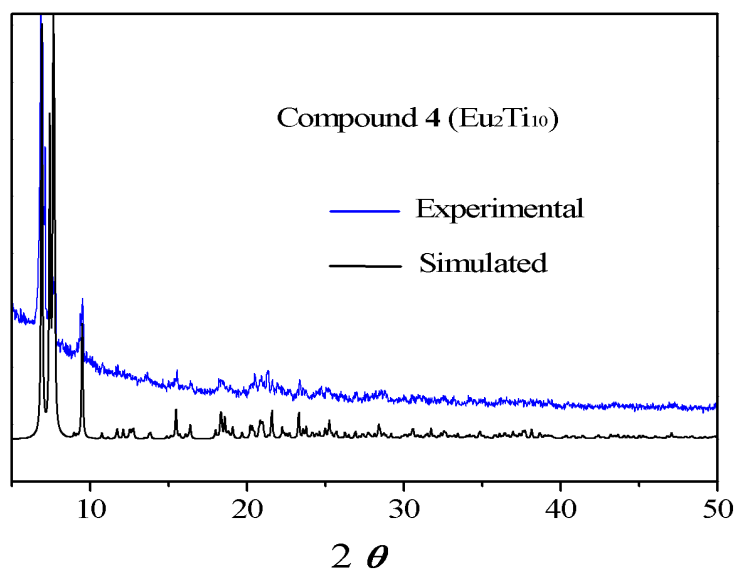
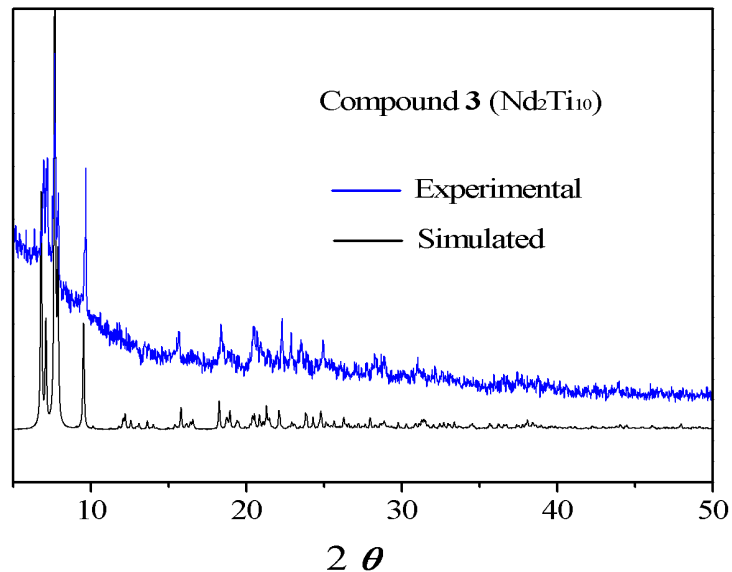


Figure S2. XRD patterns of the bulk microcrystal samples of **1–4** along with those simulated from the data of single-crystal analysis.

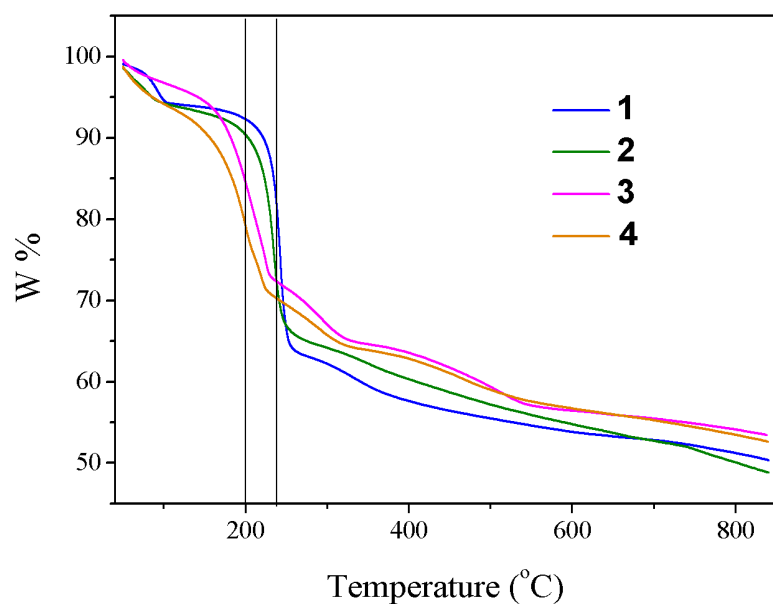
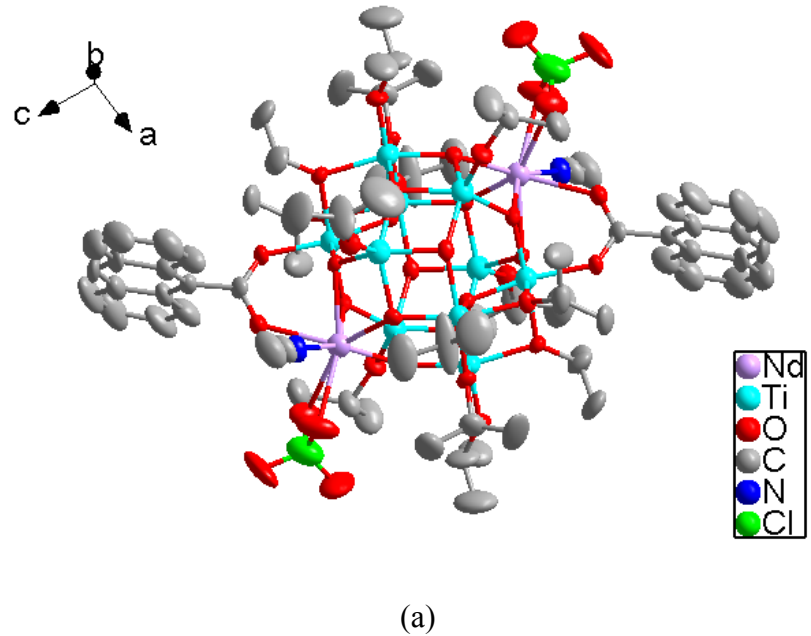
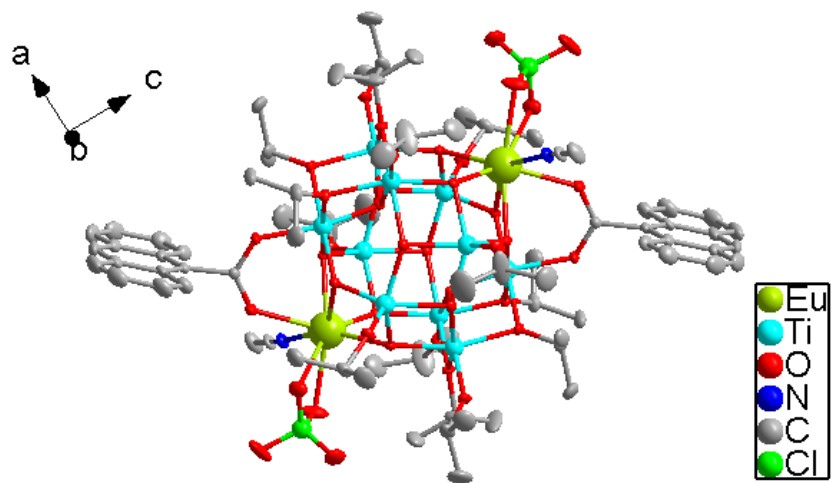


Figure S3. Thermogravimetric analysis of **1–4**.

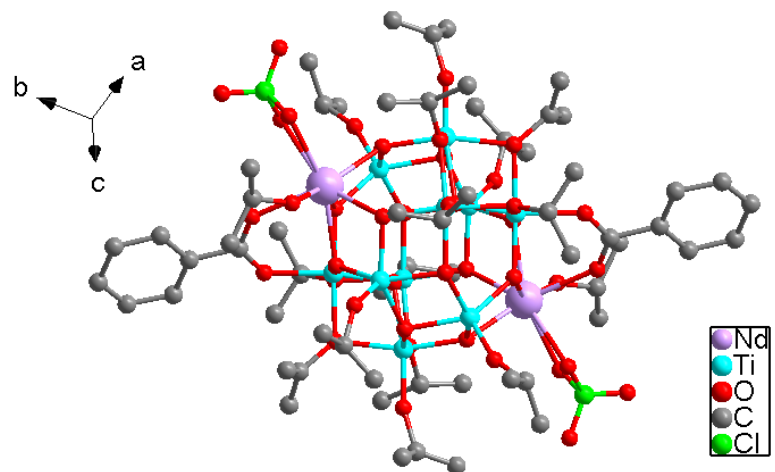


(a)

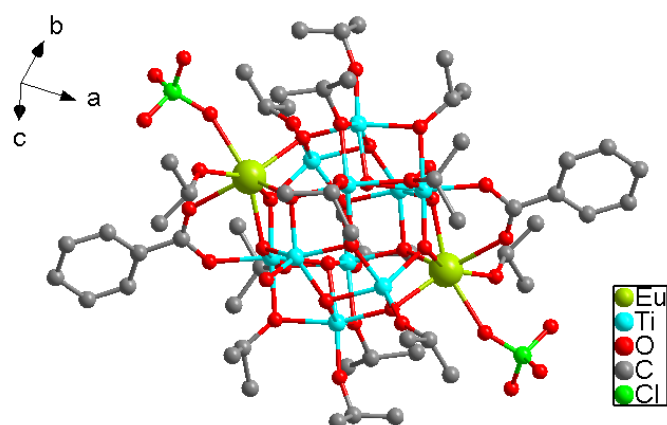


(b)

Figure S4. Molecular structures of **1** (a) and **2** (b) with the ellipsoid presentation.



(a)



(b)

Figure S5. Ball-stick structures of **3** (a) and **4** (b).

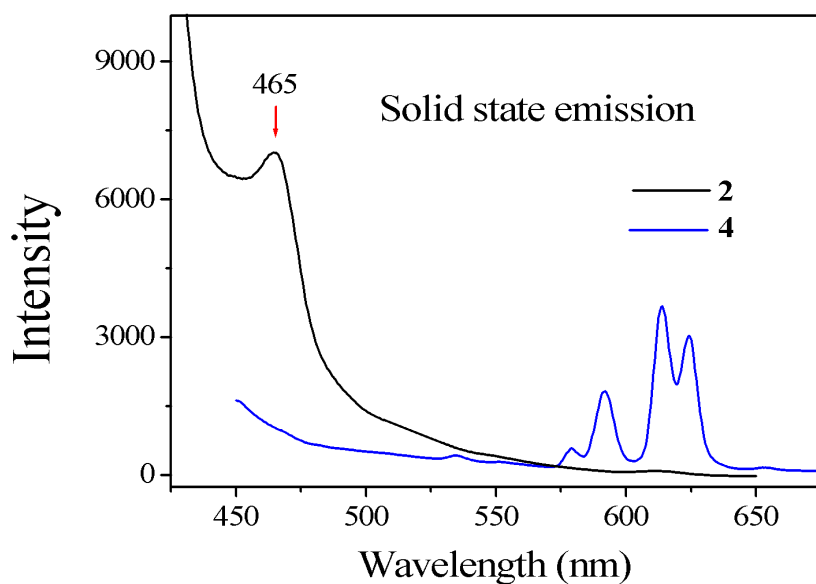


Figure S6. Solid state fluorescence spectra of **2** and **4**, also illustrating the result of energy transfer within the cluster.

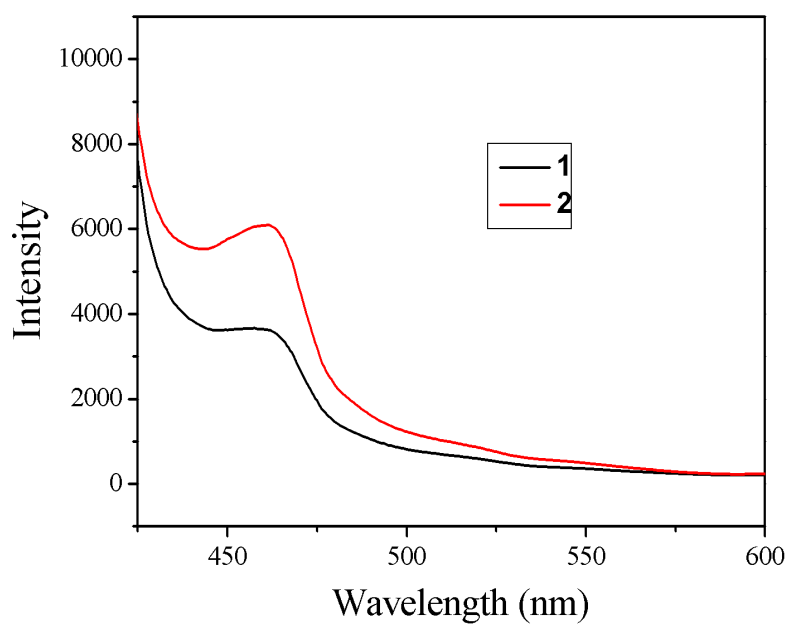


Figure S7. Solid state fluorescence spectra of **1** and **2**.